

Synthesis, X-Ray Crystal-Structure Analysis, and NMR Studies of (η^3 -Allyl)palladium(II) Complexes Containing a Novel Dihydro(phosphinoaryl)oxazine Ligand: Application in Palladium-Catalyzed Asymmetric Synthesis

by Shuangying Liu, Jürgen F. K. Müller, Markus Neuburger, Silvia Schaffner, and Margareta Zehnder*

Institut für Anorganische Chemie der Universität Basel, Spitalstrasse 51, CH-4056 Basel

The novel chiral P,N-ligand 2-[2-(diphenylphosphino)phenyl]-5,6-dihydro-4-phenyl-4*H*-1,3-oxazine (**4**) was synthesized. The corresponding [dihydro[(phosphino- κP)aryl]oxazine- κN] (η^3 -diphenylallyl)palladium(II) hexafluorophosphate **5** and the analogous [Pd(η^3 -1,3-dimethylallyl)] complex **6** were investigated by X-ray analysis and 1D- and 2D-NMR spectroscopy. The complex **5** exists as 'exo'-*syn-syn* isomer in the solid state (Fig. 1). In solution, the same isomer exceeds with 90%. The X-ray crystal structure of **6** reveals that the dihydro(phosphinoaryl)oxazine ligand coordinates in a pseudo-enantiomeric conformation compared with that of **5** (Fig. 3). A *syn-anti* arrangement of the allyl substituents of **6** is favored in the solid state. ¹H-NMR Spectroscopic investigations suggest that the auxiliary **6** adopts two conformations. This conformational instability together with 'exo'/endo' and *syn/anti* isomerization leads to the formation of 6 isomers (Fig. 4). The asymmetric allylic substitution reaction of 1,3-diphenylallyl acetate with dimethyl malonate in the presence of **4** proceeds with a selectivity of 99% ee. The ee induced by **4** in the catalytic allylic substitution of 1-methylbut-2-enyl acetate is moderate (54%).

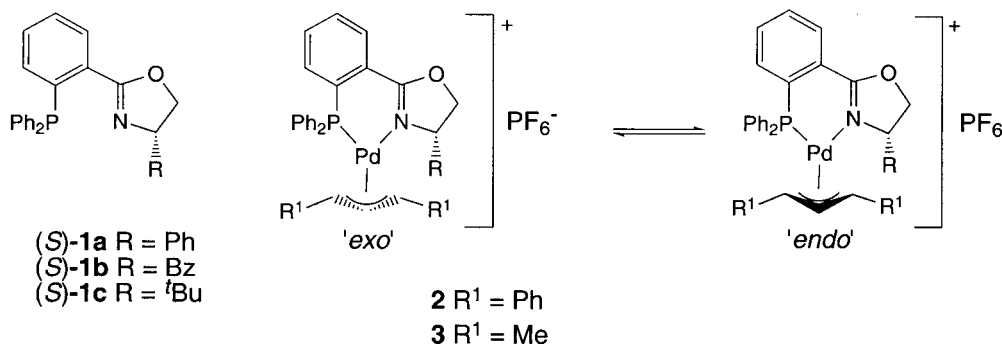
1. Introduction. – Asymmetric bidentate P,N-ligands have been successfully applied in asymmetric Pd-catalyzed allylic substitution reactions (for reviews, see [1a,b]; for selected publications, see [1c–h]). Among them, dihydro(phosphinoaryl)oxazole ligands of type **1** are effective catalysts for the enantioselective allylic substitution of 1,3-diphenylprop-2-enyl acetate, inducing selectivities of up to 99% enantiomer excess (ee) [2]. Selectivities are lower towards alkylallyl substrates, the ee values ranging between 50 and 75% [3].

In the catalytic cycle, the [Pd^{II}(η^3 -allyl)(**1**)] intermediates are considered to be crucial for the stereochemical pathway of the reaction [4]. A dependence of the configuration of the product on the [Pd^{II}(η^3 -allyl)] intermediates was reported by a number of authors. Åkermark, Vitagliano, and co-workers stabilized *anti* structures of [Pd^{II}(η^3 -allyl)] complexes with 2,9-disubstituted 1,10-phenanthroline ligands [5]. In the catalytic reaction, the configuration of the product could be controlled by the shape and the bulk of the substituents at C(2) and C(9). A correlation of the configuration of the [Pd(1,3-diphenylallyl)] moiety and that of the product was reported by Togni *et al.* in the allylic amination with [(diphenylphosphino)ferrocenyl]pyrazole catalysts [6]. The stereochemical outcome of the Pd-catalyzed amination was dependent on the formation of *syn-syn* and *syn-anti* isomers¹⁾, respectively.

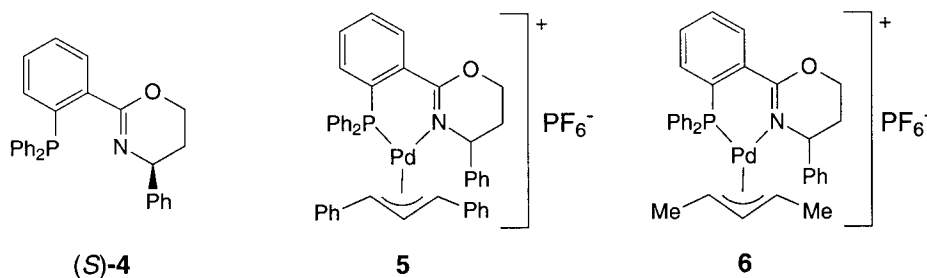
¹⁾ *syn/anti* refers to the relative position of the terminal substituents at the allyl moiety with respect to the central H-atom of the allyl moiety.

Investigations on the $[\text{Pd}^{\text{II}}(\eta^3\text{-allyl})(\mathbf{1})]\text{PF}_6$ complexes revealed that coordinated 4-monosubstituted dihydro(phosphinoaryl)oxazoles adopted a preferred conformation [4c] [7], *i.e.*, the allyl moiety adopted an 'exo' or 'endo' orientation of its central proton with respect to the substituent at C(4) of the oxazoline moiety (*Scheme 1*). In $[\text{Pd}(\eta^3\text{-PhC}_3\text{H}_3\text{Ph})(\mathbf{1})]\text{PF}_6$ complexes **2**, only a *syn-syn* arrangement of the allyl substituents was observed¹). The $[\text{Pd}(\eta^3\text{-MeC}_3\text{H}_3\text{Me})(\mathbf{1})]\text{PF}_6$ derivatives **3** showed also a *syn-anti* arrangement of the Me substituents. In solution, complexes of type **2** formed two, complexes of type **3** four interconverting cationic isomers. In every case, the most abundant species was the 'exo'-*syn-syn* isomer (*Scheme 1*).

Scheme 1. 'exo' and 'endo' Isomers. 'exo': the central C–H bond of the allyl group points towards the substituent R; 'endo': the central C–H bond points away from R.



To obtain more information on the interaction between the auxiliary and the η^3 -allyl moiety, we intended to force the chiral information closer to the allyl terminus by increasing the size of the chiral moiety. For that purpose, we chose the ligand 2-[2-(diphenylphosphino)phenyl]-5,6-dihydro-4-phenyl-4*H*-1,3-oxazine (**4**)²). The racemic complexes $[\text{Pd}^{\text{II}}(\eta^3\text{-PhC}_3\text{H}_3\text{Ph})(\mathbf{4})]\text{PF}_6$ (**5**) and $[\text{Pd}^{\text{II}}(\eta^3\text{-MeC}_3\text{H}_3\text{Me})(\mathbf{4})]\text{PF}_6$ (**6**) were prepared and their structures investigated in the solid state and in solution. The stereoselective efficiency of the (*S*)-configured novel ligand (*S*)-**4** was evaluated in the standard allylic substitution reaction [9].



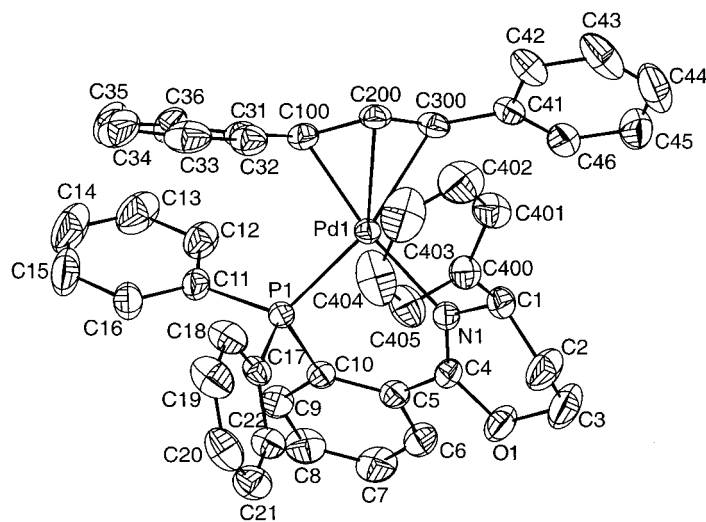
Results and Discussion. – X-Ray crystal-structure analyses of **5** and **6** were carried out. Selected geometric parameters are reported in *Table 1*. Views of the cations are given in *Figs. 1* and *2*.

²) Oxazine ligands have been applied in allylic substitution reactions [8a] and in *Heck* reactions [8b].

Table 1. Selected Geometrical Parameters [\AA , $^\circ$] for **5** and **6**. E.s.d.s in parentheses.

	5 'exo'-syn-syn	6 'endo'-syn-anti	6 'exo'-anti-syn
Bond lengths:			
Pd(1)–N(1)	2.141(2)		2.153(3)
Pd(1)–P(1)	2.258(1)		2.265(1)
Pd(1)–C(100)	2.119(3)	2.168(9)	2.014(19)
Pd(1)–C(200)	2.192(2)	2.185(6)	2.203(10)
Pd(1)–C(300)	2.345(3)	2.263(8)	2.324(17)
C(100)–C(200)	1.433(4)	1.397(8)	1.393(9)
C(200)–C(300)	1.377(4)	1.410(7)	1.376(9)
Interplanar angles:			
(allyl)/Pd–P–N/	114.3	111.9	123.2
Pd–C(100)–C(300)/Pd–P–N	21.8	8.4	6.9

Crystal Structure of 5. The coordination geometry of the cation of **5** is pseudo-square-planar. Bond lengths and bond angles are within the expected range for a $[\text{Pd}^{\text{II}}(\eta^3\text{-allyl})]$ complex. The allyl group adopts the 'exo' configuration. The substituents are in the *syn* positions¹⁾ with respect to the central proton. Due to the non-

Fig. 1. X-Ray crystal structure of the cation of **5**. Thermal ellipsoids are drawn at 30% probability.

planarity of the chelate ring of **4**, one *P*-Ph group adopts a pseudoaxial and the other a pseudoequatorial position. The dihydrooxazine substituent is in a pseudoaxial position with respect to the coordination plane. The axial Ph group and the dihydrooxazine moiety lie on the same side of the coordination plane. The cation has nearly the same chelate ring conformation as the $[\text{Pd}^{\text{II}}(\eta^3\text{-PhC}_3\text{H}_3\text{Ph})(\mathbf{1})]$ complexes.

Crystal Structure of 6. The cation of **6** shows the usual pseudo-square-planar coordination geometry. However, with respect to the geometry of the ligands, remarkable differences compared with **5** are found. The dihydro(phosphinoaryl)oxazine chelate ring adopts the inverse conformation to that of **5**. As a consequence, the

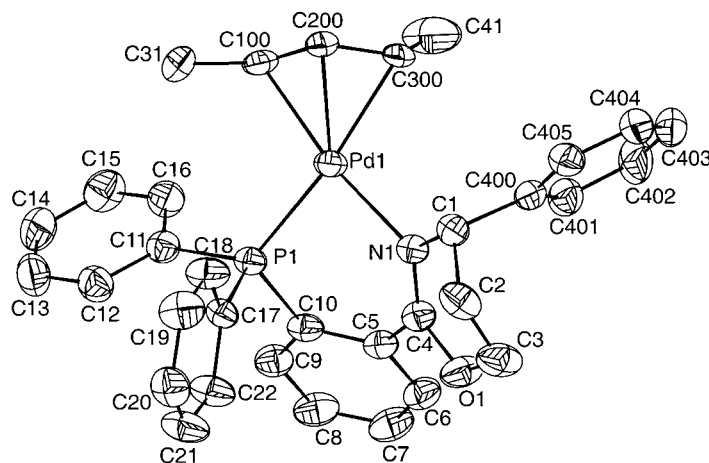


Fig. 2. X-Ray crystal structure of the cation of **6**. Thermal ellipsoids are drawn at 30% probability. For clarity, only the major isomer is shown.

dihydro(phosphinoaryl)oxazine backbone of **6** is nearly enantiomeric to that of **5**, except for the dihydrooxazine moiety (Fig. 3). The Ph substituent at the stereogenic C-atom is pseudoequatorially positioned with respect to the Pd–P–N plane. It lies in the coordination plane close to the adjacent allyl terminus.

The allyl group is disordered between ‘*exo*’ and ‘*endo*’ orientation. In both isomers, a *syn-anti* arrangement of the Me substituents is found. This is contrary to the $[\text{Pd}(\eta^3\text{-MeC}_3\text{H}_3\text{Me})(\mathbf{1})]$ complexes, in which a *syn-syn* arrangement prevails. In the more abundant isomer of **6** (60%), the *anti* Me group is the one positioned near the

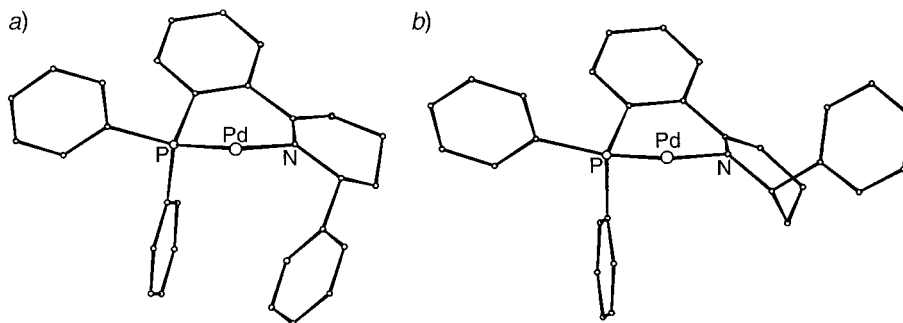


Fig. 3. Solid-state conformation of the dihydro(phosphinoaryl)oxazine ligand a) in **5** and b) in **6**

dihydrooxazine ring. In the minor isomer, the Me substituent near the phosphine moiety adopts an *anti* arrangement. A *syn-syn* arrangement of the allyl substituents would lead to severe steric interactions in both the ‘*exo*’ and ‘*endo*’ species. In the latter, the Ph substituent at C(4) of the dihydrooxazine forces the adjacent allyl Me moiety into an *anti* position. In the former, an *anti* arrangement brings the allyl Me substituent into the gap between the P-Ph groups, an arrangement which was found to be sterically favored [10].

NMR Spectroscopy of 5. The ^{31}P -NMR spectrum of **5** suggests that a mixture of three isomers is present in solution. One species predominates with *ca.* 90%. The remaining two are in low abundance of *ca.* 5%. According to the H,H coupling constants of the allyl protons, the allyl Ph substituents of the major component are in the *syn* position relative to the central allyl proton (see *Table 2*). The chemical shift of this central proton suggests that the dihydro(phosphinoaryl)oxazine adopts the same conformation in solution as in the solid state. The shielding effect of the axially positioned Ph substituent at C(4) of the dihydrooxazine moiety shifts the resonances of the central allyl proton of the 'exo' isomer to higher field relative to the corresponding signal of the 'exo' isomers of the complexes with aliphatic substituents (*ca.* 7 ppm). The chemical shifts of the minor isomers suggest the 'endo'-*syn-syn* and the 'exo'-*syn-anti* species, respectively.

NMR Spectroscopy of 6. At least six isomers of **6** exist in CDCl_3 solution. These arise from *syn-syn* or *syn-anti* positions of the allyl substituents and the 'exo'/endo' orientation of the allyl group. In addition, the dihydro(phosphinoaryl)oxazine moiety may flip between two conformations, one positioning the dihydrooxazine substituent in

Table 2. Selected ^1H -NMR Data of **5**. For numbering, see *Fig. 1*

	$\delta(\text{H})$ [ppm] ($J(\text{H,H})$ [Hz], $J(\text{H,P})$ [Hz])			$\delta(^{31}\text{P})$
	H–C(100)	H–C(300)	H–C(200)	
'exo'- <i>syn-syn</i>	3.88 ^{a)}	6.4 ^{a)}	5.72 ($J = 10.1, 14.3$)	20.95
'endo'- <i>syn-syn</i>	4.30 ($J = 11$)	4.95 ($J \approx 12$)	6.4 ^{a)}	26.12
'exo'- <i>syn-anti</i>	4.35 ($J = 12$)	6.9 ^{a)}	4.78 ($J = 8, 12$)	20.63

^{a)} Signal overlap.

a pseudoaxial and the other in a pseudoequatorial position with respect to the coordination plane. The resonances of 1D- and 2D- ^1H -NMR spectra were assigned to the isomers I–VI shown in *Fig. 4*. Selected parameters are given in *Table 3* (for numbering, see *Figs. 2* and *4*).

Table 3. ^1H -NMR Data of the Allyl Ligand of **6**. For numbering, see *Figs. 2* and *4*.

	δ [ppm] ($J(\text{H,H})$ [Hz], $J(\text{P,H})$ [Hz])				
	Me(1)	Me(3)	H–C(100)	H–C(200)	H–C(300)
I 'exo'- <i>syn-syn</i> (27%)	0.74 ($J = 6.3, 13.5$)	1.61 (br.)	3.12 (br.)	4.33 ($J = 10.3, 14.0$)	4.73
II 'endo'- <i>syn-syn</i> (19%)	0.74	1.18 ($J = 6.2, 10.3$)	3.03 ($J = 12.8, 6.0$)	5.39 ($J \approx 12$)	3.81
III 'endo'- <i>anti-syn</i> (27%)	0.30 ($J = 6.9, 6.9$)	1.84 ($J = 6.2, 11.0$)	3.78 ($J \approx 7.7$)	5.35 ($J \approx 7, 13$)	3.60
IV 'exo'- <i>syn-anti</i> (17%)	0.83 ($J = 6.3, 11.6$)	1.28 ($J = 6.0, 6.0$)	3.43 ($J = 9.8, 6.4$)	3.79	5.54 ($J \approx 7$)
V 'endo'- <i>syn-anti</i> (7%)	1.01 ($J = 9.5, 6.2$)	0.87 ($J = 6.5, 6.6$)	3.68 ($J = 6.0, 11.4$)	5.40	4.16
VI 'exo'- <i>anti-syn</i> (3%)	0.63	1.5	3.8 ^{a)}	5.2 ^{a)}	4.5 ^{a)}

^{a)} Derived from exchange cross-peaks.

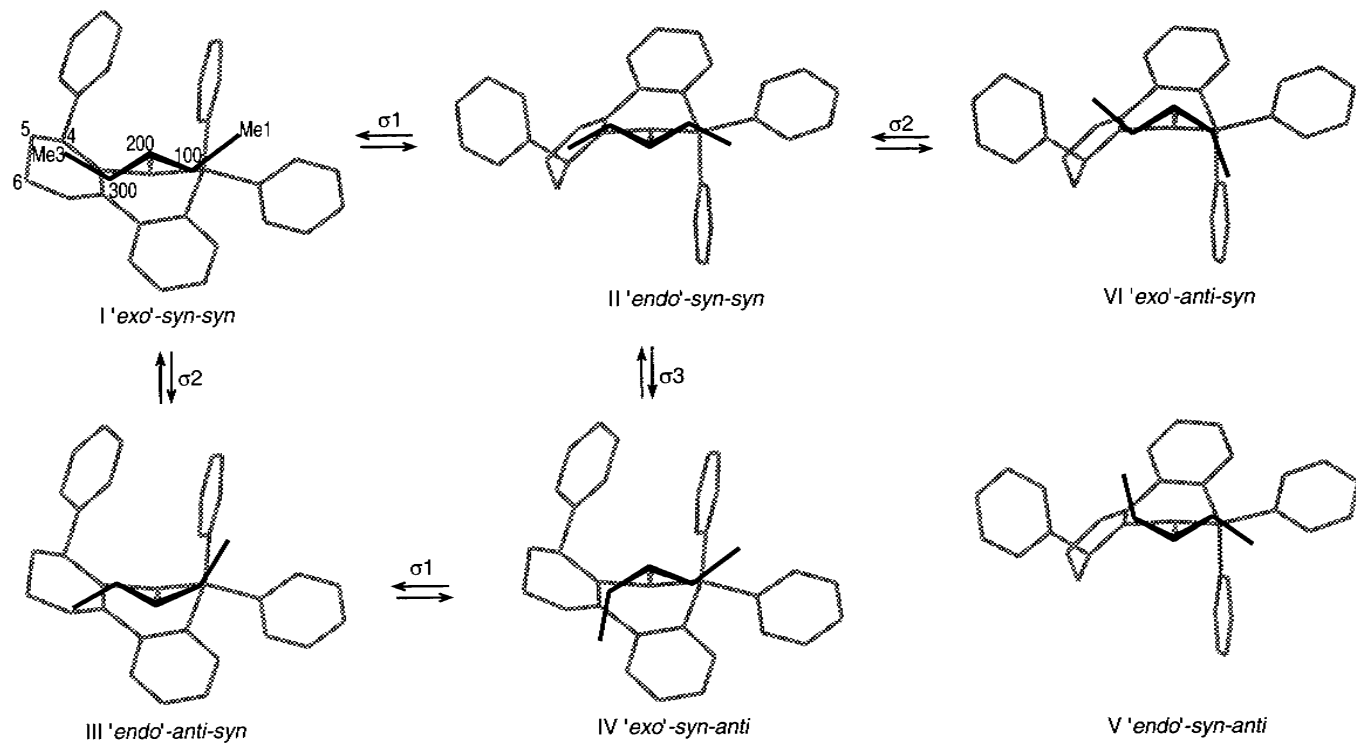


Fig. 4. Solution structures of the six isomers of **6** and exchange processes

The geometry of the allyl group was determined on the basis of the coupling patterns. Characteristically, the $^4J(\text{P,H})$ value of a *syn* Me group is larger (*ca.* 10 Hz) than that of an *anti* Me group (*ca.* 6 Hz). NOEs between H–C(100) and H–C(300) for a *syn-syn* arrangement, and between H–C(200) and Me(1) or Me(3) for a *syn-anti* or *anti-syn* arrangement, respectively, confirmed the assignment. The ‘*exo*’/‘*endo*’ orientation of the allyl group and the conformation of the dihydro(phosphinoaryl)oxazine ligand were derived from the high-field shifts of resonances of the allyl ligand due to the anisotropic ring current effect of the Ph group at C(4) of the dihydrooxazine. An axially positioned Ph group is situated above the allyl group and causes an upfield shift of the resonance of the central proton (H–C(200)) of the ‘*exo*’ isomers and of the adjacent terminal anti proton (H–C(300)) of the ‘*endo*’ isomers, respectively. An equatorial Ph group is close to the allyl terminus and affects both the H–C(300) and the Me(3) signals, but not the chemical shift of the H–C(200) resonance, independent of whether the allyl group has the ‘*exo*’ or ‘*endo*’ configuration.

Exchange cross-peaks give evidence that isomer I is in an equilibrium with isomer II and III, respectively. A $\eta^3\text{-}\eta^1\text{-}\eta^3$ mechanism is established for allyl palladium complexes. Two exchange processes are observed, *i.e.*, pseudo-rotation of the allyl group ($\sigma 1$) and a C–C rotation mechanism ($\sigma 2$). Exchange cross-peaks are observed between the corresponding protons of different allyl termini, *e.g.*, H–C(100) of isomer I and H–C(300) of isomer II, which refers to an ‘*exo*’/‘*endo*’ isomerization ($\sigma 1$).

Exchange cross-peaks are also observed between the corresponding protons of the same allyl terminus, *e.g.*, H–C(100) of I and H–C(100) of III. The Pd–C bond *trans* to P is cleaved. The ligand rotates about the C(100)–C(200) bond. The Pd–C bond is re-closed *trans* to P. The termini do not change their position relative to ligand **4**. The $\sigma 2$ process leads to a *syn/anti* exchange and an ‘*exo*’/‘*endo*’ isomerization. The exchange peaks of the $\sigma 2$ process are weaker than those of the $\sigma 1$ process. This indicates that the C–C rotation exchange is slower than the allyl rotation.

Weak exchange peaks between isomer III and IV indicate a $\sigma 1$ equilibration process. Surprisingly, an isomerization between isomer II and IV is observed, consistent with a C–C rotation mechanism similar to $\sigma 2$, but with an opening of the Pd–C bond *trans* to N.

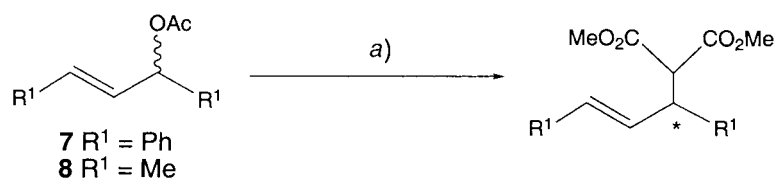
Strong exchange cross-peaks between isomer II and a further component are observed, suggesting that II is in a rapid equilibrium with isomer VI.

NMR Investigations reveal that the preferred conformation of ligand **4** (*ca.* 70%) does not correspond to its structure in the solid state. Isomers V and VI found in the solid state are only present to *ca.* 10% in solution. Evidently, the preference of the extended form of the auxiliary in the solid state is due to lattice forces. The conformation of the allyl group fits to the conformation of the dihydro(phosphinoaryl)oxazine, thus reducing the steric strain to a minimum.

Catalysis. Asymmetric allylic substitution of the allyl acetates with dimethyl malonate was carried out with the (*S*)-**4** catalyst according to the previously described method with *N,O*-bis(trimethylsilyl)acetamide (BSA) under the same conditions as with ligands **1** (*Scheme 2*). The results of the catalysis are listed in *Table 4*.

In the substitution reaction of 1,3-diphenylallyl acetate, ligand (*S*)-**4** led to a high enantioselectivity of 99%. The absolute configuration of the product suggests a preferential nucleophilic attack at the allyl terminus *trans* to P of the main ‘*exo*’-*syn-syn* isomer as in the reaction with ligands of type **1**.

Scheme 2



a) CH₂(COOMe)₂ (3 equiv.), [Pd(C₃H₅)]((*S*)-**4**)]Cl (2 mol-%), BSA (3 equiv.), KOAc (2 mol-%), CH₂Cl₂, r.t.

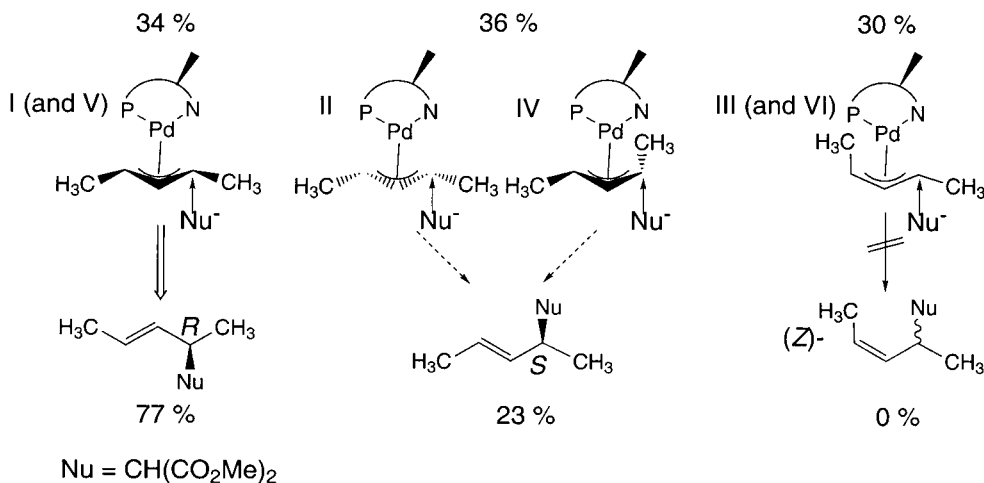
Table 4. *Enantioselective Allylic Alkylation of Acetates 7 and 8 (Scheme 2) in the Presence of (S)-4 Compared with that of (S)-1*

Ligand	Acetate	Reaction time	Yield [%]	ee Value [%]	Abs. config. ^{a)}	Ref.
(<i>S</i>)- 4	7	48 h ^{b)}	80	99	(+)-(<i>R</i>)	
(<i>S</i>)- 1a	7	1 h	99	99	(-)-(<i>S</i>)	[2]
(<i>S</i>)- 4	8	168 h ^{b)}	58	54	(+)-(<i>R</i>)	
(<i>S</i>)- 1a	8	24 h	97	50	(-)-(<i>S</i>)	[2]
(<i>S</i>)- 1c	8	24 h	96	71	(-)-(<i>S</i>)	[2]

a) See [9]. b) Reaction incomplete.

To 1-methylbutenyl acetate **8**, (*S*)-**4** induced a moderate ee value of 54%, comparable with that induced by ligand (*S*)-**1a**. The enantiomer excess does not correlate with the isomer ratio of the allyl intermediates. Isomers I and V leading to the observed product are only present to 34% (see Scheme 3). The others would give a product of opposite chirality (II and IV) or with (*Z*)-geometry (III and VI). As no (*Z*)-isomers could be detected in the substitution reaction, it is assumed that isomers III and VI do not participate in the catalytic cycle.

Scheme 3



Conclusion. – The new ligand **4** shows a high diastereoselectivity towards the η³-1,3-diphenylallyl system, leading to a preference of the ‘*exo*’-*syn*’ species. This

corresponds to an excellent asymmetric induction with an enantioselectivity of 99% ee.

Structural investigations of $[\text{Pd}^{\text{II}}(\eta^3\text{-MeC}_3\text{H}_3\text{Me})(\mathbf{4})]\text{PF}_6$ (**6**) reveal that the dihydro(phosphinoaryl)oxazine ligand lacks conformational stability. In addition, the 1,3-dimethylallyl moiety easily forms *syn-anti* isomers. The conformational lability of both the auxiliary and the allyl moiety leads to the formation of isomeric complexes. In spite of the low diastereoselectivity of ligand **4** towards the η^3 -1,3-dimethylallyl system, the enantioselectivity (54%) is marginally improved in comparison with the corresponding dihydro(phosphinoaryl)oxazole ligand **1a**. The results are in accordance with a selection mechanism proposed for ligands of type **1** [3][4], suggesting that nucleophilic attack at the allyl terminus *trans* to the P-atom of the 'exo' isomers is favored.

We thank Dr. *Gerd Scherrer* for specific NMR measurements and for helpful discussions. The support of this project by the *Swiss National Science Foundation* (project No. 20-52572.97) is gratefully acknowledged.

Experimental Part

General. Commercially available solvents and reagents were used without further purification, except for those detailed below. CH_2Cl_2 was distilled over CaH_2 under Ar. Solvents for chromatography were distilled before use. Moisture- and air-sensitive reactions were carried out under N_2 using dried glassware. The preparation of 2-(diphenylphosphino)benzotrile has been detailed in [11]. The ligand was synthesized from 2-(diphenylphosphino)benzotrile and 3-amino-3-phenylpropan-1-ol following the route of [11]. The amino alcohol was prepared according to [12]. Column chromatography (CC): SiO_2 C 560, 0.035–0.070 mm, *F* 254, *Chemische Fabrik*, Uetikon. Optical rotation: 10-cm cell at 20°, *Perkin-Elmer-141* polarimeter. NMR Spectra: when not otherwise stated, *Varian-Gemini 300*; ^1H , 300 MHz, CDCl_3 , chemical shifts δ in ppm vs. SiMe_4 (=0 ppm), coupling constants *J* in Hz; ^{31}P , 121 MHz, triphenyl phosphate as external reference (–18.0 ppm).

(\pm)-3-Amino-3-phenylpropanoic Acid. Benzaldehyde (10 g, 94 mmol), malonic acid (10.06 g, 96 mmol) and AcONH_4 (15 g) in EtOH (20 ml) were refluxed for 6 h. After cooling, the colorless solid (8.23 g) was filtered off and recrystallized from boiling H_2O : 5.27 g (34%). M.p. 220.5–221°. $^1\text{H-NMR}$ (D_2O , DCl): 6.83 (*s*, 5 arom. H); 4.15 (*dd*, *J* = 7.7, 6.7, 1 H); 2.56 (*dd*, *J* = 7.7, 17.2, 2 H); 2.45 (*dd*, *J* = 6.7, 17.2, 2 H).

(\pm)-3-Amino-3-phenylpropan-1-ol. To a stirred suspension of NaBH_4 (2.74 g, 73 mmol) in THF (30 ml), (\pm)-3-amino-3-phenylpropanoic acid (4.81 g, 9 mmol) was added. The mixture was immersed in an ice bath, and a soln. of conc. H_2SO_4 soln. (2 ml) in Et_2O (5 ml) was added dropwise. Stirring was continued at r.t. overnight. MeOH (3 ml) and 5N NaOH (140 ml) were successively added. After removal of the org. solvents, the aq. soln. was refluxed for 2 h and, after cooling, extracted with CH_2Cl_2 (3 \times 100 ml). Evaporation of the extract yielded a colorless solid (3.4 g, 89%). $^1\text{H-NMR}$: 7.20–7.37 (*m*, 5 arom. H); 4.11 (*m*, 1 H); 3.82–3.76 (*m*, 2 H); 2.75 (*br. s*, 3 H); 1.83–1.93 (*m*, 2 H).

(\pm)-Methyl 3-Amino-3-phenylpropanoate. A MeOH soln. (75 ml) of (\pm)-3-amino-3-phenylpropanoic acid (16.2 g, 100 mmol) was cooled in an ice bath. Conc. HCl soln. (18 ml) was poured slowly on the walls of the flask. The mixture was stirred for 1 h, then neutralized with sat. aq. NaHCO_3 soln., and extracted with tBuOMe . The org. phase was dried (Na_2SO_4) and evaporated: colorless oil (10.7 g, 60%). $^1\text{H-NMR}$: 7.26–7.38 (*m*, 5 arom. H); 4.43 (*t*, *J* = 6.9, 1 H); 3.68 (*s*, Me); 2.68 (*d*, *J* = 6.9, 2 H); 1.96 (*s*, 2 H).

(3*S*)-Methyl 3-Amino-3-phenylpropanoate L-Tartrate Salt. A soln. of (\pm)-methyl 3-amino-3-phenylpropanoate (23.6 g, 132 mmol) in MeOH (100 ml) was added to a boiling solution of L-tartaric acid (19.8 g, 132 mmol) in MeOH (100 ml). The product was allowed to crystallize overnight at –20°. The precipitate (15.4 g, 71%) was collected and recrystallized 3 times in MeOH (100 ml) to give an overall yield of 9.1 g (42%) of L-tartrate salt. The enantiomer excess (>98%) of a probe of recovered (*S*)-ester was measured on a *Daicel Chiralcel OD* column (λ 254 nm, hexane/*i*-PrOH 90:10, flow rate 0.3 ml/min); $t_{\text{R}}(\text{R})$ 39.3 and $t_{\text{R}}(\text{S})$ 33.3 min.

(3*S*)-Methyl 3-Amino-3-phenylpropanoate. The above crystalline L-tartrate salt (2.7 g, 8.2 mmol) was dissolved in 1N NaOH (16 ml) and CH_2Cl_2 (20 ml). The aq. phase was extracted with CH_2Cl_2 (2 \times 20 ml) and the extract dried and evaporated: colorless oil (1.26 g, 86%), which solidified in the refrigerator.

(3*S*)-3-Amino-3-phenylpropan-1-ol. (*S*)-Methyl 3-amino-3-phenylpropanoate (1.8 g, 20 mmol) was dried *in vacuo* for 3 h and added to a suspension of NaBH_4 (1.0 g, 25 mmol) in THF (10 ml). Conc. H_2SO_4 (0.66 ml) in

Et₂O (1.3 ml) were slowly added. The mixture was stirred overnight, and the (*S*)-propanol (1.29 g, 87%) was isolated as described for the (\pm)-propanol (see above).

(\pm)-2-[2-(Diphenylphosphino)phenyl]-5,6-dihydro-4-phenyl-4H-1,3-oxazine (**4**). A mixture of 2-(diphenylphosphino)benzotrile (2.00 g, 7.0 mmol), (\pm)-3-amino-3-phenylpropan-1-ol (1.26 g, 7.6 mmol), and ZnCl₂ (0.95 g, 7.0 mmol) in chlorobenzene (20 ml) under N₂ was heated to reflux for 94 h. The mixture was submitted to CC (4 × 5 cm, silica gel; with CH₂Cl₂/hexane 1:2 (100 ml; removal of benzotrile), then AcOEt): **4** (0.83 g, 28%). Colorless solid. TLC (AcOEt/hexane): R_f 0.5. ¹H-NMR: 7.83–7.86 (*m*, 1 arom. H); 7.09–7.46 (*m*, 17 arom. H); 6.88–6.92 (*m*, 1 arom. H); 4.53 (*dd*, *J* = 4.9, 7.7, 1 H); 4.06–4.09 (*m*, 2 H); 1.91–2.00 (*m*, 1 H); 1.59–1.70 (*m*, 1 H). ¹³C-NMR (75 MHz, CDCl₃): 157.8 (C(2)); 143.4, 138.5, 138.3, 138.2, 138.0, 137.5, 137.2 (arom. C); 134.0, 133.7, 129.8, 129.2, 128.4, 128.3, 128.1, 126.6 (arom. CH); 63.3 (C(6)); 54.4 (C(4)); 29.2 (C(5)). ³¹P-NMR: –6.19. FAB-MS: 422 (100), 344 (19), 317 (23), 304 (48), 289 (21), 183 (29), 117 (45), 105 (21).

(4*S*)-2-[2-(Diphenylphosphino)phenyl]-5,6-dihydro-4-phenyl-4H-1,3-oxazine ((*S*)-**4**). As described for **4**, with 2-(diphenylphosphino)benzotrile (1.0 g, 3.5 mmol), (3*S*)-3-amino-3-phenylpropan-1-ol (0.7 g, 3.8 mmol) and ZnCl₂ (0.53 g, 3.5 mmol): 0.42 g (28%) of (*S*)-**4**. Colorless solid.

(\pm)-[2-[2-(Diphenylphosphino- α P)phenyl]-5,6-dihydro-4-phenyl-4H-1,3-oxazine- α N]](η^3 -1,3-diphenylprop-2-enyl)palladium(II) Hexafluorophosphate (**5**). A mixture of [PdCl(η^3 -diphenylallyl)]₂ (100 mg, 0.15 mmol) and **4** (140 mg, 0.3 mmol) in EtOH (10 ml) was stirred for 1.5 h. The resulting soln. was treated with (NH₄)PF₆ (80 mg). After 10 min, the yellow precipitate (250 mg, 97%) was filtered off. Recrystallization from CH₂Cl₂/EtOH/hexane 1:3:3 afforded air-stable crystals suitable for X-ray analysis. ¹H-NMR (for numbering, see Fig. 4; major isomer) 8.28–8.33 (*m*, 1 arom. H); 6.88–7.72 (*m*, 22 arom. H); 6.35–6.44 (*m*, H–C(300); 2 arom. H); 6.14–6.22 (*m*, 4 arom. H); 5.72 (*dd*, *J* = 14.3, 10.1, H–C(200)); 4.42–4.50 (*m*, 1 H–C(6)); 4.19–4.26 (*m*, 1 H–C(6)); 3.85–3.90 (*m*, H–C(100), H–C(4)); 1.90–1.99 (*m*, 1 H–C(5)); 1.44–1.55 (*m*, 1 H–C(5)). ³¹P-NMR: 20.95 (major); 26.17 (minor); 20.63 (minor).

(\pm)-[2-[2-(Diphenylphosphino- α P)phenyl]-5,6-dihydro-4-phenyl-4H-1,3-oxazine- α N]](η^3 -methylbut-2-enyl)-palladium(II) Hexafluorophosphate (**6**). A suspension of [PdCl(η^3 -MeC₃H₃Me)]₂ (80 mg, 0.2 mmol) and of **4** (170 mg, 0.4 mmol) was stirred in EtOH (5 ml) for 1 h. The resulting pale yellow soln. was treated with (NH₄)PF₆ and the precipitate collected on a filter and recrystallized from EtOH. ¹H-NMR (600 MHz, CDCl₃; for numbering, see Fig. 4): isomer I: 8.13–8.18 (*m*, 1 arom. H); 7.11–7.80 (*m*, 16 arom. H); 6.81–6.94 (*m*, 2 arom. H); 5.05 (*dd*, *J* = 4.9, 7.7, H–C(4)); 4.67–4.76 (*m*, 1 H–C(6)); 4.35–4.39 (*m*, 1 H–C(6)); 4.32 (*dd*, *J* = 10.3, 14.0, H–C(200)); 3.07–3.16 (*m*, H–C(100)); 2.15–2.17 (*m*, 1 H–C(5)); 1.58–1.65 (*m*, 1 H–C(5), 1 Me); 0.74 (*dd*, *J* = 6.3, 13.5, 1 Me); isomer II: 8.02–8.04 (*m*, 1 arom. H); 7.11–7.80 (*m*, 16 arom. H); 7.05–7.06 (*m*, 2 arom. H); 5.39 (*dd*, *J* ≈ 12, H–C(200)); 5.16–5.20 (*m*, H–C(4)); 4.34–4.38 (*m*, 1 H–C(6)); 4.12–4.17 (*m*, 1 H–C(6)); 3.77–3.81 (*m*, H–C(300)); 3.03 (*dq*, *J* = 12.8, 6.0, H–C(100)); 1.72–1.77 (*m*, 1 H–C(5)); 1.32–1.38 (*m*, 1 H–C(5)); 1.18 (*dd*, *J* = 6.2, 10.3, 1 Me); 0.74 (*dd*, 1 Me); isomer III: 8.13–8.18 (*m*, 1 arom. H); 7.11–7.80 (*m*, 16 arom. H); 6.81–6.94 (*m*, 2 arom. H); 5.35 (*dd*, *J* ≈ 7, 13, H–C(200)); 4.96 (*dd*, *J* = 4.8, 10.3, H–C(4)); 4.78–4.83 (*m*, 1 H–C(6)); 4.51–4.54 (*m*, 1 H–C(6)); 3.78 (*m*, *J* ≈ 7.7, H–C(100)); 3.60 (*ddq*, H–C(300)); 2.36–2.38 (*m*, 1 H–C(5)); 1.83 (*dd*, *J* = 11.0, 6.2, 1 Me); 1.64–1.69 (*m*, 1 H–C(5)); 0.30 (*t*, *J* = 6.9, 1 Me); isomer IV: 8.23–8.25 (*m*, 1 arom. H); 7.11–7.80 (*m*, 16 arom. H); 6.72–6.74 (*m*, 2 arom. H); 5.54 (*sext.*, *J* ≈ 7, H–C(300)); 5.10 (*dd*, *J* = 4.7, 10.3, H–C(4)); 4.85–4.90 (*m*, 1 H–C(6)); 4.49–4.51 (*m*, 1 H–C(6)); 3.77–3.81 (*dd*, H–C(200)); 3.43 (*dq*, *J* = 9.8, 6.4, H–C(100)); 2.27–2.30 (*m*, 1 H–C(5)); 1.64–1.71 (*m*, 1 H–C(5)); 1.28 (*t*, *J* = 6.0, 1 Me); 0.83 (*dd*, *J* = 6.3, 11.6, 1 Me); isomer V: 7.96–7.98 (*m*, 1 arom. H); 6.6–7.80 (*m*, 18 arom. H); 5.35–5.41 (*m*, H–C(200)); 5.25–5.26 (*m*, H–C(4)); 4.14–4.18 (*m*, H–C(300)); 3.68 (*dq*, *J* = 6.0, 11.4, H–C(100)); 1.01 (*dd*, *J* = 9.5, 6.2, 1 Me); 0.87 (*dd*, *J* = 6.5, 6.6, 1 Me); isomer VI: 1.5 (*dd*, 1 Me); 0.63 (*dd*, 1 Me).

³¹P-NMR: 27.42 (7%); 25.70 (19%); 23.41 (27%); 23.32 (17%); 23.24 (3%); 18.93 (27%).

Palladium-Catalyzed Allylic Alkylation of 1,3-Diphenylprop-2-enyl Acetate Using the BSA Procedure. A mixture of [Pd(C₃H₃)Cl]₂ (2.4 mg, 6.6 μmol) and (*S*)-**4** (6.7 mg, 15.9 μmol) in CH₂Cl₂ (0.6 ml) was stirred for 30 min at r.t. To the resulting pale-yellow mixture, a soln. of *rac*-1,3-diphenylprop-2-enyl acetate (160.3 mg, 0.64 mmol) in CH₂Cl₂ (3 ml) was added. Then dimethyl malonate (252 mg, 1.9 mmol), *N,O*-bis(trimethylsilyl)-acetamide (388 mg, 1.90 mmol), and AcOK (1.1 mg) were added. The mixture was stirred at r.t. for 48 h. Traces of starting material were detected by TLC (hexane/AcOEt 3:1). R_f (starting material) 0.45, R_f (product) 0.33. The soln. was diluted with Et₂O (25 ml) and washed twice with ice cold sat. aq. NH₄Cl soln. The org. phase was dried (Na₂SO₄) and evaporated. CC (SiO₂; hexane/AcOEt 3:1) afforded 165 mg (80%) of colorless *dimethyl 2-[(E)-1,3-diphenylprop-2-enyl]propanedioate*. Chiral CC (*Daicel Chiralcel OD* column, λ = 254 nm, hexane/ⁱPrOH 99:1, flow rate 0.3 ml/min): t_R(*R*) 38.40, t_R(*S*) 40.88 min; 99% ee for (*R*)-enantiomer. ¹H-NMR: 7.19–7.32 (*m*, 10 arom. H); 6.49 (*d*, *J* = 15.6, H–C(3′)); 6.33 (*dd*, *J* = 8.4, 15.8, H–C(2′)); 4.27 (*dd*, *J* = 8.4, 10.7, H–C(1′)); 3.95 (*d*, *J* = 10.8, H–C(2)); 3.70 (*s*, Me); 3.51 (*s*, Me).

Palladium-Catalyzed Allylic Alkylation of 1-Methylbut-2-enyl Acetate Using the BSA Procedure. A mixture of $[\text{Pd}(\text{C}_5\text{H}_5\text{Cl})_2]$ (2.4 mg, 6.6 μmol) and (*S*)-**4** (6.7 mg, 15.9 μmol) in CH_2Cl_2 (0.6 ml) was stirred for 30 min at r.t. To the resulting pale-yellow mixture, a soln. of 1-methylbut-2-enyl acetate (81.1 mg, 0.635 mmol) in CH_2Cl_2 (3 ml) was added. Then, dimethyl malonate (252 mg, 1.9 mmol), *N,O*-bis(trimethylsilyl)acetamide (388 mg, 1.90 mmol), and AcOK (1.1 mg) were added. The mixture was stirred at r.t. for 65 h. After that time, a considerable amount of starting material was detected by TLC (hexane/AcOEt 4 : 1): R_f (starting material) 0.48, R_f (product) 0.39. The soln. was diluted with CH_2Cl_2 (25 ml) and washed twice with ice cold sat. aq. NH_4Cl soln. The org. phase was dried (Na_2SO_4) and evaporated. CC (SiO_2 ; hexane/AcOEt 4 : 1) afforded 50 mg (39%) of dimethyl 2-[(*E*)-1-methylbut-2-enyl]propanedioate. $[\alpha]_D^{25} = +14.9$ ($c = 1.23$, CHCl_3). $^1\text{H-NMR}$: 5.51 (*ddq*, $J = 15.2, 6.4, 0.8$, $\text{H}-\text{C}(3'')$); 5.34 (*ddq*, $J = 15.2, 8.1, 1.3$, $\text{H}-\text{C}(2'')$); 3.69, 3.73 (2*s*, 2 Me); 3.27 (*d*, $J = 9.1$, $\text{H}-\text{C}(2)$); 2.83–2.96 (*m*, $\text{H}-\text{C}(1')$); 1.63 (*dd*, $J = 6.4, 1.3$, Me(4')); 1.06 (*d*, $J = 6.8$, Me–C(1')). $^1\text{H-NMR}$ (CDCl_3 , 300 MHz, 0.5 equiv. of $[\text{Eu}(\text{hfc})_3]$): Splitting of Me–C(1') signal; 53% ee for the (*R*)-enantiomer.

A second experiment following the same procedure was carried out. After 148 h, the reaction was still incomplete. CC yielded 0.74 g (58%), ee 54%.

*X-Ray Crystal-Structure Analyses*³). Crystal data and parameters of the data collection are compiled in Table 5. Unit-cell parameters were determined by accurate centering of 25 strong reflections. Reflection

Table 5. Experimental Conditions for the X-Ray Crystal-Structure Analysis of **5** and **6**

	5	6
Chemical formula	$\text{C}_{43}\text{H}_{37}\text{F}_6\text{NOP}_2\text{Pd} \cdot 0.5 (\text{C}_6\text{H}_{14})$	$\text{C}_{33}\text{H}_{33}\text{F}_6\text{NOP}_2\text{Pd}$
M_r	909.2	742.0
Crystal size [mm]	$0.30 \times 0.40 \times 0.46$	$0.08 \times 0.36 \times 0.52$
a [Å]	11.497(1)	10.638(1)
b [Å]	14.225(3)	11.515(1)
c [Å]	25.858(5)	14.228(2)
α [°]	90	80.71(1)
β [°]	91.94(1)	73.49(1)
γ [°]	90	79.46(1)
V [Å ³]	4227(1)	1631.7(4)
Crystal system	monoclinic	triclinic
Space group	$P2_1/c$	$P-1$
Z	4	2
$F(000)$	1860	752
Radiation	MoK_α (λ 0.71069 Å)	MoK_α (λ 0.71069 Å)
Temperature [K]	293	293
Calc. density [g/cm ³]	1.43	1.51
Abs. coeff. [mm ⁻¹]	0.57	0.72
Scan type	$\omega/2\theta$	$\omega/2\theta$
θ_{max} [°]	30.44	30.44
No of measured refl. ^{a)}	10978	8221
No. of independent refl.	10351	7929
No. of refl. in ref. $I \geq 3\sigma(I)$	7600	5343
No. of parameters	606	509
Final R [%]	3.51	4.51
Final R_w [%]	4.38	4.87
Last max./min. in diff. map	0.54/–0.39	0.79/–0.48
Weighting scheme	<i>Chebyshev</i> polynomial [17]	

^{a)} Without reflections flagged weak by the data-collection software.

³⁾ Crystallographic data (excluding structure factors) for the structures reported in this paper have been deposited with the *Cambridge Crystallographic Date Centre* as deposition No. CCDC-139777 and CCDC-139778. Copies of the data can be obtained, free of charge, on application to the CDCC, 12 Union Road, Cambridge CB21EZ, UK (fax: +44(1223)336 033; e-mail: deposit@ccdc.cam.ac.uk).

intensities were collected on a four-circle diffractometer (*Enraf-Nonius CAD4*). Three standard reflections were monitored every hour during data collection. The usual corrections were applied. The absorption correction was determined using φ scans [13]. The structures were solved by direct methods [14]. Anisotropic least-squares refinement against F was carried out on all non-H-atoms using the program CRYSTALS [15]. The positions of the H-atoms were calculated. Scattering factors were taken from the International Tables of Crystallography, Vol. IV. Figs. 1–3 were designed with the program SNOOPI [16]. The anions of **5** and **6**, and the allyl ligand of **6** were found to be disordered. The disordered atoms were refined in two positions holding the sum of their occupancies equal to one. Geometric restraints were applied to the disordered parts of the structure during the structure refinement.

REFERENCES

- [1] a) B. M. Trost, D. L. Van Vranken, *Chem. Rev.* **1996**, *96*, 395; b) G. Helmchen, *J. Organomet. Chem.* **1999**, *576*, 203; c) H. Kubota, K. Koga, *Tetrahedron Lett.* **1994**, *35*, 6689; d) P. Wimmer, M. Widhalm, *Tetrahedron: Asymmetry* **1995**, *6*, 657; e) J.-M. Valk, T. D. W. Claridge, J. M. Brown, D. Hibbs, M. B. Hursthouse, *Tetrahedron: Asymmetry* **1995**, *6*, 2597; f) K. H. Ahn, C.-W. Cho, J. Park, S. Lee, *Tetrahedron: Asymmetry* **1997**, *8*, 1179; g) I. Achiwa, A. Yamazaki, K. Achiwa, *Synlett* **1998**, 45; h) B. Gläser, H. Kunz, *Synlett* **1998**, 53.
- [2] P. von Matt, A. Pfaltz, *Angew. Chem.* **1993**, *105*, 614; *Angew. Chem., Int. Ed.* **1993**, *32*, 566; P. von Matt, Ph. D. Thesis, University of Basel, 1993; J. Sprinz, G. Helmchen, *Tetrahedron Lett.* **1993**, *34*, 1769; G. J. Dawson, C. G. Frost, J. M. J. Williams, S. J. Coote, *Tetrahedron Lett.* **1993**, *34*, 3149.
- [3] J. V. Allen, S. J. Coote, G. J. Dawson, C. G. Frost, C. J. Martin, J. M. J. Williams, *J. Chem. Soc., Perkin Trans. I* **1994**, 2065; P. von Matt, O. Loiseleur, G. Koch, A. Pfaltz, C. Lefeber, T. Feucht, G. Helmchen, *Tetrahedron: Asymmetry* **1994**, *5*, 573; G. Helmchen, S. Kudis, P. Sennhenn, H. Steinhagen, *Pure Appl. Chem.* **1997**, *69*, 513.
- [4] a) C. G. Frost, J. Howarth, J. M. J. Williams, *Tetrahedron: Asymmetry* **1992**, *3*, 1089; b) O. Reiser, *Angew. Chem.* **1993**, *105*, 576; *Angew. Chem., Int. Ed.* **1993**, *32*, 547; c) J. Sprinz, M. Kiefer, G. Helmchen, M. Reggelin, G. Huttner, O. Walter, L. Zsolnai, *Tetrahedron Lett.* **1994**, *35*, 1523; d) J. M. Brown, D. I. Hulmes, P. J. Guiry, *Tetrahedron* **1994**, *50*, 4493; e) A. Pfaltz, *Acta Chem. Scand.* **1996**, *50*, 189.
- [5] M. Sjögren, S. Hansson, P.-O. Norrby, B. Åkermark, M. E. Cucciolito, A. Vitalgiano, *Organometallics* **1992**, *11*, 3954.
- [6] A. Togni, U. Burckhardt, V. Gramlich, P. S. Pregosin, R. Salzmänn, *J. Am. Chem. Soc.* **1996**, *118*, 1031.
- [7] N. Baltzer, L. Macko, S. Schaffner, M. Zehnder, *Helv. Chim. Acta* **1996**, *79*, 803; L. Macko, Ph.D. Thesis, University of Basel, 1996; S. Schaffner, L. Macko, M. Neuburger, M. Zehnder, *Helv. Chim. Acta* **1997**, *80*, 463; S. Liu, J. F. K. Müller, M. Neuburger, S. Schaffner, M. Zehnder, *J. Organomet. Chem.* **1997**, *549*, 283; S. Schaffner, J. F. K. Müller, M. Neuburger, M. Zehnder, *Helv. Chim. Acta* **1998**, *81*, 1223.
- [8] a) P. A. Evans, T. A. Brandt, *Tetrahedron Lett.* **1996**, *37*, 9143; b) E. P. Kündig, P. Meier, *Helv. Chim. Acta* **1999**, *82*, 1360.
- [9] a) U. Leutenegger, G. Umbricht, C. Fahrni, P. von Matt, A. Pfaltz, *Tetrahedron* **1992**, *48*, 2143; B. M. Trost, T. J. Dietsche, *J. Am. Chem. Soc.* **1973**, *95*, 8200.
- [10] P. Barbaro, P. S. Pregosin, R. Salzmänn, A. Albinati, R. W. Kunz, *Organometallics* **1995**, *14*, 5160.
- [11] G. Koch, G. C. Lloyd-Jones, O. Loiseleur, A. Pfaltz, R. Prétôt, S. Schaffner, P. Schnider, P. von Matt, *Recl. Trav. Chim. Pays-Bas* **1995**, *114*, 206.
- [12] T. B. Johnson, J. E. Livak, *J. Am. Chem. Soc.* **1936**, *58*, 299; H. H. Wasserman, G. D. Berger, *Tetrahedron* **1983**, *39*, 2459; A. Abiko, S. Masamune, *Tetrahedron Lett.* **1992**, *33*, 5517.
- [13] A. C. T. North, D. C. Phillips, F. S. Mathews, *Acta Crystallogr., Sect. A* **1968**, *24*, 351.
- [14] A. Altomare, M. C. Burla, M. Camalli, G. Cascarano, C. Giacovazzo, A. Gualgiardi, G. Polidori, 'SIR92', *J. Appl. Crystallogr.* **1994**, *27*, 435.
- [15] D. Watkin, 'Crystals, Issue 9', Chemical Crystallography Laboratory, Oxford, 1990.
- [16] K. Davies, P. Braid, B. Foxman, H. Powell, 'SNOOPI', Oxford University, 1989.
- [17] J. R. Carruthers, D. J. Watkin, *Acta Crystallogr., Sect. A* **1979**, *35*, 698.

Received February 1, 2000